

Dynamic characteristics estimation from the ambient vibration of existing bridge by realization theories

Md. Rajab ALI*, Toshihiro OKUMATSU**, Takatoshi OKABAYASHI ***, and Bashir Ahmed JAWAID****

*M. of Eng., Graduate student, Nagasaki University, Bunkyo machi 1-14, Nagasaki 852-8521

**Dr. of Eng., Assistant Professor, Dept. of Civil Eng., Nagasaki University, Bunkyo machi 1-14, Nagasaki 852-8521

***Dr. of Eng., Professor, Dept. of Civil Eng., Nagasaki University, Bunkyo machi 1-14, Nagasaki 852-8521

****M. of Eng., Graduate student, Nagasaki University, Bunkyo machi 1-14, Nagasaki 852-8521

An automatic estimation system for bridge dynamic characteristics (frequency, damping ratio, and vibration mode) under ambient vibration by ERA, ERA/DC and PHCA method is presented in this paper. The Hankel matrix was derived from block covariance of ambient vibration data. The experiments were conducted under (a) strong wind, (b) weak wind and (c) under traffic condition to estimate the dynamic characteristics of existing steel langer girder bridge. As a result of this study, the better result is realized from the strong wind data. In contrast, the inducement of high frequency by the data under traffic condition leads to frequent estimation of higher mode with inconsistent level of accuracy. In the various method of analysis, ERA/DC method has the advantages for its simple algorithm and ability to provide accurate estimation with fast calculation speed.

Keywords: ambient vibration, system identification, dynamic characteristics estimation, realization theory

1. INTRODUCTION

The maintenance and management of bridge structures is a critical issue to maintain their safe and effective functioning. Hence, various technologies and systems were developed for bridge health diagnosis¹⁻³. In among the conventional methods, structural health diagnosis methods by the estimation of dynamic characteristics under ambient vibration have been developing⁴⁻⁶. The advantage in this technique is the measurement of naturally available ambient vibration. On the other hand, the degradation of bridge health condition are time being factor. In addition, for large structures, like bridge, the quantity of damage is generally very small that cannot be easily identified. Concerning this problem, an automatic, accurate estimation of bridge dynamic characteristics can facilitate us to accumulate periodic information about their health condition to do long term monitoring.

Several different approaches have been proposed to develop a system of estimating the bridge dynamic characteristics under ambient vibration. Accordingly, dynamic characteristics of

bridges were estimated from the single point and multipoint measurement of ambient vibration⁷⁻⁹ using time domain modal analysis^{10, 11}, ARMA model¹², deterministic and stochastic realization theories¹³⁻²¹. However, these systems are still beset with considerable challenges. Especially, the ambient vibration behavior such as wind velocity, and moving vehicles have significant influence on the estimation accuracy²².

This paper presents an automatic, high accurate estimation method for bridge dynamic characteristics considering various condition of ambient vibration by realization theories. From the block covariance of ambient vibration data, bridge dynamic characteristics (frequency, damping ratio and vibration mode) were estimated using three different realization theories. The selected theories are, ERA (Eigensystem Realization Algorithm) method proposed by J. N. Juang²³, ERA method with the aid of data correlation fit known as ERA/DC (ERA with Data Correlations) proposed by J. N. Juang²⁴. Another method about the estimation process of system matrix by shifting the observability matrix, proposed by J. N. Juang¹⁷ can be mentioned as PHCA (Principal Hankel Component Algorithm)

method. In those methods the Hankel matrix was generalized by random distribution of Markov parameters derived from the free decay response. In this study, the generalized Hankel matrix was derived from the block covariance of ambient vibration data, which is the basic feature of ERA, ERA/DC, and PHCA methods.

These methods were applied to the ambient vibration measurement of the existing steel longer girder bridge for demonstrating the applicability. The field measurements were conducted under three different condition of ambient vibration mentioned, namely, (a) strong wind (b) weak wind and (c) under traffic condition. The effectiveness of automatic estimation was critically evaluated using measured ambient vibration data. The better result is achieved from the strong wind ambient vibration data. In contrast, the data under traffic condition induced high frequency leads to frequent estimation of higher mode but do not show consistency since the excitation is not steady in nature. Among the studied methods, ERA/DC method exhibited better performance due to the simplicity of its algorithm.

2. HANKEL MATRIX BY BLOCK COVARIANCE MATRIX

A bridge structure can be modeled by finite element method and its dynamic behavior is expressed by n -dof system equation of motion, where the external forces applied to the r node among n node.

$$\mathbf{m}\ddot{\mathbf{z}}(t) + \mathbf{c}\dot{\mathbf{z}}(t) + \mathbf{k}\mathbf{z}(t) = \mathbf{d}\mathbf{w}(t) \quad (1)$$

where, $\mathbf{z}(t) \in \mathbf{R}^n$ and $\mathbf{w}(t) \in \mathbf{R}^r$ are the displacement and external force vector. $\mathbf{m} \in \mathbf{R}^{n \times n}$, $\mathbf{c} \in \mathbf{R}^{n \times n}$ and $\mathbf{k} \in \mathbf{R}^{n \times n}$ are the mass, general viscous damping, and stiffness matrix respectively, and $\mathbf{d} \in \mathbf{R}^{n \times r}$ is external input force applied on r node.

To represent the state space form of the Eq.(1), introducing the state variable $\mathbf{x}(t) \in \mathbf{R}^{2n}$ as follows:

$$\mathbf{x}(t) = \begin{bmatrix} \mathbf{z}(t) \\ \dot{\mathbf{z}}(t) \end{bmatrix} \quad (2)$$

Using Eq.(2) and considering m -point observation vector as $\mathbf{y}(t) \in \mathbf{R}^m$, the continuous time state space form of Eq.(1) are

$$\dot{\mathbf{x}}(t) = \bar{\mathbf{A}}\mathbf{x}(t) + \bar{\mathbf{B}}\mathbf{w}(t) \quad (3-1)$$

$$\mathbf{y}(t) = \bar{\mathbf{C}}\mathbf{x}(t) \quad (3-2)$$

where, $\bar{\mathbf{A}} \in \mathbf{R}^{2n \times 2n}$, $\bar{\mathbf{B}} \in \mathbf{R}^{2n \times r}$ are defined by

$$\bar{\mathbf{A}} = \begin{bmatrix} \mathbf{c} & \mathbf{m} \\ \mathbf{m} & \mathbf{0} \end{bmatrix}^{-1} \begin{bmatrix} -\mathbf{k} & \mathbf{0} \\ \mathbf{0} & \mathbf{m} \end{bmatrix}, \bar{\mathbf{B}} = \begin{bmatrix} \mathbf{c} & \mathbf{m} \\ \mathbf{m} & \mathbf{0} \end{bmatrix}^{-1} \begin{bmatrix} \mathbf{d} \\ \mathbf{0} \end{bmatrix} \quad (4)$$

and $\bar{\mathbf{C}} \in \mathbf{R}^{m \times 2n}$ is introduced from observed value $\mathbf{y}(t)$ which is extracted from state variable $\mathbf{x}(t)$.

In vibration measurement, the observation signals are discretized by sampling time T . Hence, the continuous state equation can be represent by discretized state equation. Change of $\mathbf{w}(t)$ is assumed to be gradual for $\mathbf{t}_k \leq \tau \leq \mathbf{t}_{k+1} = \mathbf{t}_k + T$ and we can write.

$$\mathbf{w}(t) = \mathbf{w}(t = t_k) = \mathbf{w}(k) \quad (t_k \leq \tau \leq t_{k+1}) \quad (5)$$

and $\mathbf{x}(t = t_k) = \mathbf{x}(k)$. Thus the Eq.(1) is to be transformed into the following discretized state equations.

$$\mathbf{x}(k+1) = \mathbf{A}\mathbf{x}(k) + \mathbf{B}\mathbf{w}(k) \quad (6-1)$$

$$\mathbf{y}(k) = \mathbf{C}\mathbf{x}(k) \quad (6-2)$$

whereas the coefficient matrices \mathbf{A} and \mathbf{B} for Eq.(8) are as follows:

$$\mathbf{A} = e^{\bar{\mathbf{A}}T}, \quad \mathbf{B} = (e^{\bar{\mathbf{A}}T} - \mathbf{I})\bar{\mathbf{A}}^{-1}\bar{\mathbf{B}} \quad (7)$$

notably, $\mathbf{A} \in \mathbf{R}^{2n \times 2n}$, $\mathbf{B} \in \mathbf{R}^{2n \times r}$, and observation matrix $\mathbf{C} \in \mathbf{R}^{m \times 2n} = \bar{\mathbf{C}}$.

By applying the random vibration theory, a special solution to the Eqs.(6-1) and (6-2) is estimated. In this process, the covariance of zero-mean white noise $\mathbf{w}(k) \in \mathbf{R}^r$ is written as

$$\mathbf{E}[\mathbf{w}(k+l)\mathbf{w}^T(l)] = \begin{cases} \Sigma_{\mathbf{w}} & (l=0) \\ 0 & (l \neq 0) \end{cases} \quad (8)$$

where, $\mathbf{E}[\]$ is mathematical expectation and $\Sigma_{\mathbf{w}} \in \mathbf{R}^{r \times r}$. For a stationary stochastic process, the covariance of solution process is the time lag function of $\mathbf{x}(l+k)$ and $\mathbf{x}(l)$. For $k \rightarrow \infty$, covariance of the solution process $\mathbf{R}_x(k) = \mathbf{E}[\mathbf{x}(k)\mathbf{x}^T(k)] = \mathbf{R}_x$. Hence, with the aid of Eqs.(6-1) and (8) autocorrelation of the solution process can be written as

$$\mathbf{R}_{xx}(k) = \mathbf{E}[\mathbf{x}(l+k)\mathbf{x}^T(l)] = \mathbf{A}^k \mathbf{R}_x \quad (l \geq 0) \quad (9)$$

By the same process, covariance matrix $\mathbf{R}_{yy}(k)$ of observation data is formulated by the Eqs.(6-2) and (9).

$$\mathbf{R}_{yy}(k) = \begin{cases} \mathbf{C}\mathbf{R}_x\mathbf{C}^T & k=0 \\ \mathbf{C}\mathbf{A}^{k-1}\hat{\mathbf{B}} & k>1 \end{cases} \quad (10)$$

where, $\hat{\mathbf{B}} = \mathbf{R}_x\mathbf{C}$. The expression $\mathbf{R}_{yy}(k)$ is same as Markov parameters.

3. STOCHASTIC REALIZATION THEORIES

3.1 System identification by ERA method

ERA method was developed by Ho-Kalman and applied by Juang¹⁷⁾ for modal analysis where the Hankel matrix was generalized by impulse response function. In the following process, the ERA method is introduced from the covariance of ambient vibration data. If τ is the data sampling time in discrete time T , m -dimensional observation vector $\mathbf{y}(k)$ yields the covariance matrix as

$$\mathbf{R}_{yy}(k) = \mathbf{E}[\mathbf{y}(\tau)\mathbf{y}^T(k+\tau)] \quad (\tau=1, \dots, N) \quad (11)$$

Hankel matrix is derived from the block covariance matrix as

$$\mathbf{H}(k) = \begin{bmatrix} \mathbf{R}_{yy}(k) & \dots & \mathbf{R}_{yy}(k+l-1) \\ \mathbf{R}_{yy}(k+1) & \dots & \mathbf{R}_{yy}(k+l) \\ \vdots & \ddots & \vdots \\ \mathbf{R}_{yy}(k+s-1) & \dots & \mathbf{R}_{yy}(k+s+l-2) \end{bmatrix} \quad (12)$$

where, $\mathbf{H}(k) \in \mathbf{R}^{(m \times s) \times (m \times l)}$ and s, l representing the integer that determines the size of Hankel matrix. The Hankel matrix can be decomposed by the substitution of covariance matrix stated in Eq.(10) into Eq.(12), since it is formulated from the covariance of observed value.

$$\mathbf{H}(k-1) = \begin{bmatrix} \mathbf{C} \\ \mathbf{C}\mathbf{A} \\ \vdots \\ \mathbf{C}\mathbf{A}^{s-1} \end{bmatrix} \mathbf{A}^{k-1} \begin{bmatrix} \hat{\mathbf{B}} & \mathbf{A}\hat{\mathbf{B}} & \dots & \mathbf{A}^{l-1}\hat{\mathbf{B}} \end{bmatrix} = \mathbf{P}_\rho \mathbf{A}^{k-1} \mathbf{Q}_\rho \quad (13)$$

where, block matrices \mathbf{P}_p and \mathbf{Q}_q are the expanded observability and expanded controllability matrices respectively, while the rank of the system matrix \mathbf{A} is $n \times n$. The singular value decomposition of Hankel matrix stated in Eq.(13) for $k=1$ yields

$$\mathbf{H}(0) = \mathbf{U}\mathbf{S}\mathbf{V}^T = \mathbf{P}_p \mathbf{Q}_q \quad (14)$$

where, \mathbf{U} and \mathbf{V} are orthogonal matrices, and \mathbf{S} is rectangular matrix. With the aid of Eq.(14) it is logical to write

$$\mathbf{P}_p = \mathbf{U}_n \mathbf{S}_n^{\frac{1}{2}} \quad \text{and} \quad \mathbf{Q}_q = \mathbf{S}_n^{\frac{1}{2}} \mathbf{V}_n^T. \text{Eq.(12) for } k=2 \text{ becomes}$$

$$\mathbf{H}(1) = \mathbf{P}_p \mathbf{A} \mathbf{Q}_q \quad (15)$$

Thus system matrix \mathbf{A} is calculated by using Eq.(15). The observation matrix \mathbf{C} is calculated from the first m rows of \mathbf{P}_p while the external force matrix $\hat{\mathbf{B}}$ generates from the first r rows of \mathbf{Q}_q .

$$\mathbf{A} = \mathbf{S}_n^{-\frac{1}{2}} \mathbf{U}_n^T \mathbf{H}(1) \mathbf{V}_n \mathbf{S}_n^{-\frac{1}{2}} \quad (16)$$

$$\mathbf{C} = \mathbf{E}_m^T \mathbf{U}_n \mathbf{S}_n^{\frac{1}{2}} \quad (17)$$

$$\hat{\mathbf{B}} = \mathbf{S}_n^{\frac{1}{2}} \mathbf{V}_n^T \mathbf{E}_r \quad (18)$$

Coefficient matrices \mathbf{A} , $\hat{\mathbf{B}}$ and \mathbf{C} by ERA method are thus calculated. Here, \mathbf{E}_m and \mathbf{E}_r are defined by

$$\mathbf{E}_m^T = [\mathbf{I}_m \quad \mathbf{0}_m \dots \mathbf{0}_m], \quad \mathbf{E}_r^T = [\mathbf{I}_r \quad \mathbf{0}_r \dots \mathbf{0}_r] \quad (19)$$

$\mathbf{0}_i$ and \mathbf{I}_i are $(i \times i)$ zero and identity matrices, respectively.

3.2 System identification by ERA/DC method

The development of ERA method was further proposed by Juang¹⁸⁾ through data correlation fit to solve the deterministic realization problem. For the case of stochastic realization, it can be proposed with the aid of Eqs.(13) and (14). The advantage of this method is $(m \times p) \times (m \times q)$ dimensional square matrix, which is formulated from the correlation of covariance matrix for m -point observation.

$$\mathbf{R}_{RR}(k-1) = \mathbf{H}(k-1)\mathbf{H}(0)^T = \mathbf{P}_p \mathbf{A}^{k-1} \mathbf{Q}_q \mathbf{Q}_q^T \mathbf{P}_p^T = \mathbf{P}_p \mathbf{A}^{k-1} \tilde{\mathbf{Q}}_c \quad (20)$$

$$\tilde{\mathbf{Q}}_c = \mathbf{Q}_q \mathbf{Q}_q^T \mathbf{P}_p^T = \mathbf{Q}_q \mathbf{H}(0)^T \quad (21)$$

The dimension of covariance matrix $\mathbf{R}_{RR}(k-1)$ is smaller than Hankel matrix $\mathbf{H}(k-1)$. Especially, this effect is large enough when the number of rows in Hankel matrix is large. In this method, coefficient matrices \mathbf{A} , $\tilde{\mathbf{Q}}_c$ and \mathbf{P}_p are computed from $\xi \times \eta$ block covariance correlation matrix followed by the similar process of ERA method, which is defined by

$$\mathbf{H}_R(k-1) = \begin{bmatrix} \mathbf{R}_{RR}(k-1) & \dots & \mathbf{R}_{RR}(k+\eta-1) \\ \vdots & & \vdots \\ \mathbf{R}_{RR}(k+\xi-1) & \dots & \mathbf{R}_{RR}(k+(\xi+\eta)-1) \end{bmatrix} \\ = \mathbf{P}_\xi \mathbf{A}^{k-1} \mathbf{Q}_\eta \quad (22)$$

where, matrices \mathbf{P}_ξ and \mathbf{Q}_η are the extended block correlation observability and extended block correlation controllability matrix, respectively. Now we can find the $\mathbf{H}_R(0)$ from Eq.(22) for $k=1$ and executing singular value decomposition similar to ERA method which yields

$$\mathbf{H}_R(0) = \mathbf{P}_\xi \mathbf{Q}_\eta = \bar{\mathbf{U}}_n \bar{\mathbf{S}}_n^{\frac{1}{2}} \bar{\mathbf{S}}_n^{\frac{1}{2}} \bar{\mathbf{V}}_n^T \quad (23)$$

where, $\mathbf{P}_\xi = \bar{\mathbf{U}}_n \bar{\mathbf{S}}_n^{\frac{1}{2}}$ and $\mathbf{Q}_\eta = \bar{\mathbf{S}}_n^{\frac{1}{2}} \bar{\mathbf{V}}_n^T$. Using the Eqs.(15) and (15), the coefficient matrices are estimated as

$$\mathbf{A} = \bar{\mathbf{U}}_n \bar{\mathbf{S}}_n^{-\frac{1}{2}} \mathbf{H}_R(1) \bar{\mathbf{V}}_n^T \bar{\mathbf{S}}_n^{-\frac{1}{2}} \quad (24)$$

$$\mathbf{C} = \mathbf{E}_m \mathbf{P}_p \quad (25)$$

where, \mathbf{P}_p is the upper $m \times p$ rows of \mathbf{P}_ξ . The notation $\tilde{\mathbf{Q}}_c$ is calculated from the upper $r \times q$ rows of \mathbf{Q}_η and \mathbf{Q}_q can be calculated by using Eq.(21) while $\hat{\mathbf{B}}$ is calculated using Eq.(19) to yield the following equation.

$$\hat{\mathbf{B}} = \mathbf{Q}_q \mathbf{E}_r \quad (26)$$

Stochastic realization problem thus can be solved by ERA/DC method.

3.3 PHCA (Principal Hankel Component Algorithm) method

This method was originally proposed by J. N. Juang¹⁷⁾. Expanded observability matrix \mathbf{P}_p and expanded controllability matrix \mathbf{Q}_q can be presented by the decomposition of block Hankel matrix $\mathbf{H}(0)$ as stated in Eq.(15). Defining $\mathbf{P}_p^{\uparrow m}$ as the matrix formed by deleting the first m rows of \mathbf{P}_p and $\mathbf{P}_p^{\downarrow m}$ as the matrix formed by deleting the last m rows of \mathbf{P}_p , i.e.,

$$\mathbf{P}_p^{\uparrow m} = \begin{bmatrix} \mathbf{C} \mathbf{A} \\ \vdots \\ \mathbf{C} \mathbf{A}^{p-2} \\ \mathbf{C} \mathbf{A}^{p-1} \end{bmatrix} = \mathbf{U}_n^{\uparrow m} \mathbf{S}_n^{\frac{1}{2}}, \quad \mathbf{P}_p^{\downarrow m} = \begin{bmatrix} \mathbf{C} \\ \vdots \\ \mathbf{C} \mathbf{A} \\ \mathbf{C} \mathbf{A}^{p-2} \end{bmatrix} = \mathbf{U}_n^{\downarrow m} \mathbf{S}_n^{\frac{1}{2}} \quad (27)$$

In this case, $\mathbf{U}_n^{\downarrow m}$ and $\mathbf{U}_n^{\uparrow m}$ are determined by deleting the last and first m rows of \mathbf{U}_n , respectively. Thus the next relationships are derived from Eq.(27).

$$\mathbf{U}_n^{\downarrow m} \mathbf{S}_n^{\frac{1}{2}} \mathbf{A} = \mathbf{U}_n^{\uparrow m} \mathbf{S}_n^{\frac{1}{2}} \quad (28)$$

which leads to

$$\mathbf{A} = \mathbf{S}_n^{-\frac{1}{2}} \left[\mathbf{U}_n^{\downarrow m} \right]^\dagger \mathbf{U}_n^{\uparrow m} \mathbf{S}_n^{\frac{1}{2}} \quad (29)$$

where, $[\]^\dagger$ is known as general pseudo inverse. The estimation procedure for observation matrix \mathbf{C} , and external force matrix $\hat{\mathbf{B}}$ are the same as mentioned in Eq.(17) and (18). Thus PHCA method can be proposed to estimate \mathbf{A} , $\hat{\mathbf{B}}$ and \mathbf{C} matrices by stochastic realization.

4. DYNAMIC CHARACTERISTICS ESTIMATION

4.1 Eigenvalue and eigenvector

The eigenvalue analysis of coefficient matrix \mathbf{A} (which is derived in Eqs.(16), (24) and (29)) generates the dynamic properties of the system since it characterizes the systems dynamic properties. In the process, the complex conjugate eigenvalues corresponds the frequencies and damping ratio while eigenvectors relate to the vibration mode. The following equation represents the complex conjugate eigenvalues.

$$\lambda_k = X_{\text{Re}}^k \pm X_{\text{Im}}^k \quad (30)$$

Frequencies and damping ratio are obtained from the real and

imaginary part of complex eigenvalues from the following equations.

$$h_k \omega_k = -1 / \Delta \log \sqrt{X_{\text{Re}}^k{}^2 + X_{\text{Im}}^k{}^2} \quad (31)$$

$$\omega_k \sqrt{1 - h_k^2} = 1 / \Delta \tan^{-1}(X_{\text{Im}}^k / X_{\text{Re}}^k) \quad (32)$$

where, Δ is data sampling time. In the following process, the observation was done for sampling point to estimate the vibration modes from all modes of structural system. If we denote the eigenmatrix of the coefficient matrix \mathbf{A} as $\mathbf{\Phi}$ the estimated vibration modes for sampling points are

$$\hat{\mathbf{\Phi}} = \mathbf{C}\mathbf{\Phi} \quad (33)$$

The estimated modes and frequencies follow the same order of vibration.

4.2 Model rank²⁵⁾

For the case of system identification, the determination of the model rank with the help of noise information criteria is very important and the studied methods can handle that problem effectively through the singular value decomposition. The singular value decomposition allows to arrange the singular values in decreasing order and the lower singular values are numerically zero or nearly equal to zero, which is considered as noise. In case of the absolutely noise free data, there should be a big drop in numerical values between the two singular value matrices $\mathbf{S}' = \text{diag}(\sigma_1 \cdots \sigma_n)$ $\sigma_1 \geq \sigma_2 \cdots \sigma_n \geq 0$ and $\mathbf{S}'' = \text{diag}(\sigma_{n+1} \cdots \sigma_p)$ $\sigma_{n+1} \geq \sigma_{n+2} \cdots \sigma_p \geq 0$, for this case, the rank of state space model is easily identifiable. But practically the significant gap may not be observed due to the noise corruption. Hence, the element number of \mathbf{S}' is to be chosen sufficiently large to avoid the under estimated model rank. Thus, inspection of the singular values might help us to select model rank n such that $\sigma_n \gg \sigma_{n+1}$.

4.3 Dynamic characteristics extraction process

Although a minimum rank system matrix is estimated as shown in Eqs.(16), (24), and (29), another challenge still have to be overcome for ambient vibration measurement. The estimated eigenvalues from the coefficient matrix \mathbf{A} , possesses dynamic properties of structural system, external force characteristics and some other noise which cannot be separated easily. In this circumstance, the eigenvalues are displayed on a complex plane as shown in Figure 1 and the boundary conditions are applied to separate the eigenvalues related to structural dynamic behavior. The boundary conditions can be formulated as well. For proportional damping system, the eigenvalues of system matrix

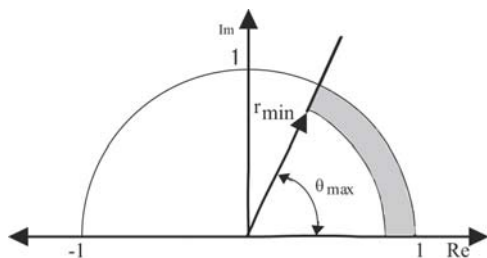


Fig.1 Existence limit of structural eigenvalues

\mathbf{A} can also be expressed by the following equation.

$$\lambda_k = e^{-h_k \omega_k T} (\cos \omega_{dk} T + i \sin \omega_{dk} T) \quad (34)$$

We can derive another relation by polar coordinate system on complex plane by considering $\omega_{dk} \cong \omega_k$ for small values of damping ratio.

$$r = e^{-h_k \omega_k T}, \theta = \tan^{-1} \omega_{dk} T \cong \tan^{-1} \omega_k T \quad (35)$$

For the purpose of extracting the eigenvalues related to system dynamic properties, the upper limit of frequency and damping are restricted as ω_{max} and h_{max} respectively, and the boundary condition established such that

$$r_{\text{min}} < r < 1 \quad (36)$$

$$0 < \theta < \theta_{\text{max}} \quad (37)$$

where, $r_{\text{min}} = e^{-h_{\text{max}} \omega_{\text{max}} T}$ and $\theta_{\text{max}} = \tan^{-1} \omega_{\text{max}} T$. The shaded area covered by $r_{\text{min}}, \theta_{\text{max}}$ is considered as the allowable region for the existence of system eigenvalues. Thus the eigenvalues which are exist within the shaded area should be extracted to estimate the frequency and damping ratio using Eq.(31) and (32).

The eigenvectors are also extracted followed by the same sequence of selected eigenvalues to find the vibration modes of m - point observation corresponding to p order extracted frequencies that can be mathematically expressed as

$$\hat{\mathbf{\Phi}} = \begin{bmatrix} \phi_{11} & \cdots & \phi_{1p} \\ \vdots & \ddots & \vdots \\ \phi_{m1} & \cdots & \phi_{mp} \end{bmatrix} \quad (38)$$

5. AMBIENT VIBRATION MEASUREMENT

5.1 The Kabashima bridge

The steel langer girder bridge (Kabashima Bridge), situated in Nagasaki city has been selected for this study as an object bridge (Figure 2) to estimate its dynamic characteristics. Table 1 explains history and properties of selected Bridge.



Fig.2 Kabashima bridge

Table 1 Details of Kabashima bridge

Bridge Type	Steel langer girder bridge
Length	227m (152m)
width	7.5m
Construction year	1986

5.2 Experiments

To carry out the ambient vibration measurements on the existing steel langer girder bridge, accelerometers were placed at various locations along the bridge length. Five accelerometers were setup at 25.50 m interval on the girder as shown in the Figure 3. The instruments used for the experiments are listed on Table 2. The measurement was conducted in different time under various conditions. Sixty Thousands (60,000) data for every channel were observed and recorded in 10 minutes. The acceleration signals is converted from analogue to digital data by AD converter card (DAQ Card), and recorded by the personal computer. Virtual measurement instrument software Lab VIEW was used as a measurement software. The dynamic characteristics (frequency, damping, and vibration mode) were estimated by processing the measured acceleration data after conducting the measurements.

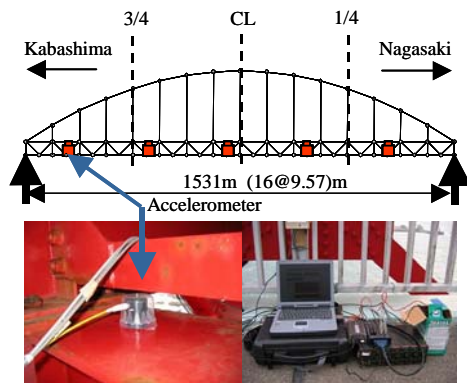


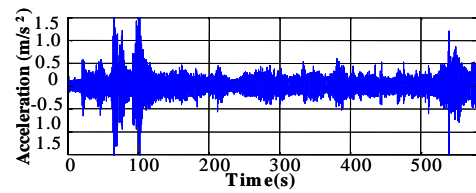
Fig.3 Experiment set up for multipoint ambient vibration measurement

Table 2 Experiment equipments

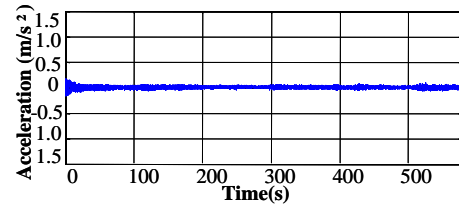
Device	Type(manufacturer)	Specifications
A/D converter	DAC card-6062E (National Instruments)	Analog Input: 16ch, 12 bit
Accelerometer	710 (TEAC)	Sensitivity: 300 (mv/m/s ²) Frequency response : 0.02-200Hz
Amplifier	SA-611(TEAC)	
Personal computer	CF-19 (Panasonic)	OS: Windows XP Pro

5.3 Characteristics of measured data

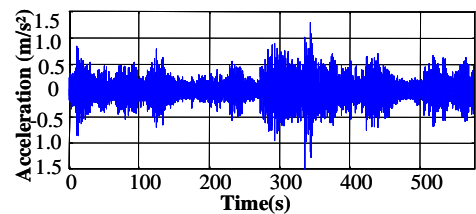
The experiments were conducted under three different ambient conditions to measure the various type of ambient vibration response. The data represent in Figure 4(a) is measured under strong windy condition, whereas Figure 5(a) shows the respective power spectrum density. It can be seen from the figures that during the experiment the bridge was vibrating under high amplitude with uniform intensity. Figures 4(b) and 5(b) are the representation of the experimental data, which is taken under weak wind condition. The data characteristics revealed that the bridge was responding uniformly with low



(a) Acceleration response (strong wind)

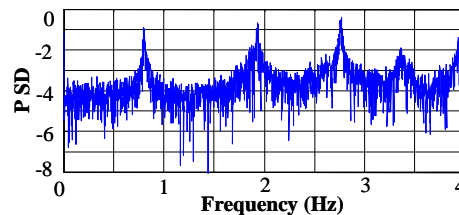


(b) Acceleration response (weak wind)

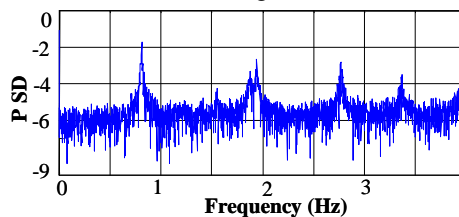


(c) Acceleration response (under traffic condition)

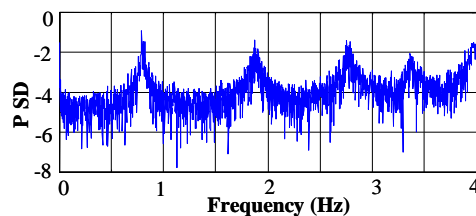
Fig.4 Experiment data



(a) Strong wind



(b) Weak wind



(c) under traffic condition

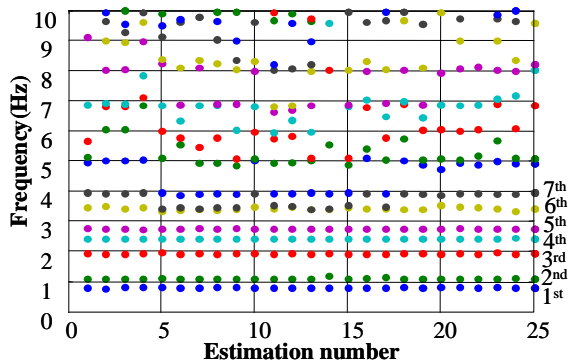
Fig.5 Power spectrum density of experiment data

amplitude. Another experiment was conducted under traffic condition, in this case the bridge was exciting well but the amplitude of vibration is non-stationary as shown in Figures 4(c) and 5(c).

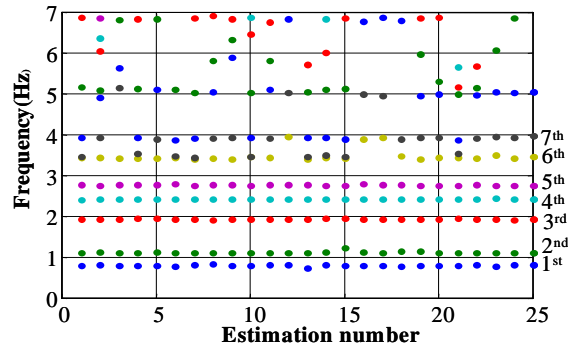
5.4 Data processing system (Formation of Hankel matrix)

The selection of number of block rows and block columns has significant effect on estimation accuracy. Too small number of block rows and block column results in poor accuracy on dynamic characteristics estimation. On the other hand, selection of large values of block rows and block column increase the computational load remarkably. That is why, an optimum size of Hankel matrix is needed for better realization. In general, the number of rows in Hankel matrix should be comparatively large and normally recommended as 10 to 12 times of the number of observation point. The sufficiently large number of block column in Hankel matrix leads to stable estimation. In this study, the optimum size of Hankel matrix was considered as $(5 \times 55) \times (5 \times 200)$. One thousand and two hundred (1200) data were analyzed to estimate each set of dynamic characteristics and the calculation were continuously done for 25 times.

6. DYNAMIC CHARACTERISTICS ESTIMATION



(a) Maximum frequency limit 10 Hz



(b) Maximum frequency limit 7 Hz

Fig.6 Estimated frequency by ERA/DC method (strong wind)

(STRONG WIND)

6.1 Frequency

The frequencies are estimated by ERA, ERA/DC and PHCA method from the experimental data measured under strong wind condition. With an aim to investigate the influence of the frequency limit on estimation accuracy, the estimated frequency by ERA/DC method can be shown in Figures 6(a) and 6(b)

Table 3 Accuracy evaluation (strong wind)

Mode Order	Frequency(Hz)			
	Mean	Std.	C.V.(%)	
1 st	ERA	0.914	0.147	16.03
	ERA/DC	0.914	0.147	16.03
	PHCA	0.964	0.177	18.32
2 nd	ERA	1.349	0.303	22.45
	ERA/DC	1.349	0.303	22.45
	PHCA	1.353	0.402	29.73
3 rd	ERA	2.001	0.273	13.61
	ERA/DC	2.001	0.273	13.61
	PHCA	2.047	0.382	18.67
4 th	ERA	2.571	0.240	9.33
	ERA/DC	2.571	0.240	9.33
	PHCA	2.699	0.316	11.71
5 th	ERA	3.110	0.474	15.21
	ERA/DC	3.110	0.474	15.21
	PHCA	3.191	0.678	21.25
6 th	ERA	3.855	0.610	15.83
	ERA/DC	3.855	0.610	15.83
	PHCA	3.997	0.731	18.31
7 th	ERA	4.326	0.703	16.24
	ERA/DC	4.326	0.703	16.24
	PHCA	4.571	0.678	14.84

where the maximum frequency was limited by 10Hz, and 7Hz respectively. It can be clearly seen that same performance on automatic estimation is realized and accuracy remains unchanged up to first seven modes for both cases. It is concluded that more than 4 Hz frequencies cannot be estimated with good accuracy even though the maximum frequency limit changes from 7Hz to 10 Hz. The results of the estimated frequency derived from ERA, ERA/DC and PHCA methods are presented in Table 3 for comparison. Since the steady estimation is possible only for first seven modes, the mean frequencies, standard deviations, and the coefficients of variations are compared in the following sections up to seventh mode only. Table shows that PHCA method realized comparatively higher mean values as compared to other two methods. Table 3 reveals that the coefficient of variation for ERA and ERA/DC is within 2% except seventh mode, which is less than coefficient of variation in PHCA method.

6.2 Damping ratio

The damping ratio is automatically estimated by ERA, ERA/DC and PHCA method, and the results from ERA/DC

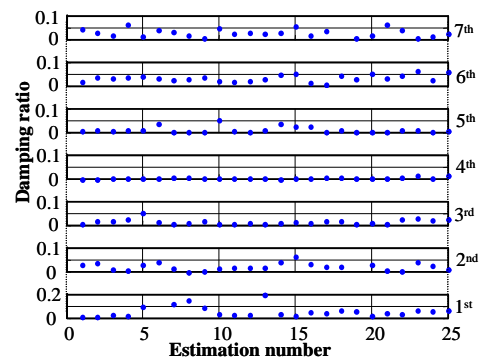


Fig.7 Estimated damping ratio by ERA/DC method (strong wind)

method are graphically represented in Figure 7. Although the level of consistency for individual method is quite different, it appears to be steady realization on automatic estimation. The accuracy of estimation were accomplished by various methods has shown in Table 4. The table reveals that comparatively higher damping values are estimated by PHCA method whereas the realized percentage of coefficient of variation was lower than other two methods. The coefficient of variation is less than 90 percent except first and second mode for all three methods. The coefficient of variation is within 128 percent up to second mode. The causes of the estimation of higher values by PHCA method might be due to some unpredictable computational errors.

Table 4 Accuracy evaluation (strong wind)

Mode Order	Damping ratio			
	Mean	Std.	C.V. (%)	
1 st	ERA	0.0679	0.0359	52.83
	ERA/DC	0.0679	0.0359	52.83
	PHCA	0.1934	0.0613	31.68
2 nd	ERA	0.0499	0.0236	47.37
	ERA/DC	0.0499	0.0236	47.37
	PHCA	0.1996	0.0714	35.77
3 rd	ERA	0.0298	0.0253	84.85
	ERA/DC	0.0298	0.0253	84.85
	PHCA	0.1051	0.0279	26.49
4 th	ERA	0.0299	0.0206	68.77
	ERA/DC	0.0299	0.0206	68.77
	PHCA	0.0890	0.0436	48.54
5 th	ERA	0.0233	0.0172	73.83
	ERA/DC	0.0233	0.0172	73.83
	PHCA	0.0685	0.0324	47.37
6 th	ERA	0.0274	0.0146	53.33
	ERA/DC	0.0274	0.0146	53.33
	PHCA	0.0581	0.0199	34.35
7 th	ERA	0.0212	0.0128	60.62
	ERA/DC	0.0212	0.0128	60.62
	PHCA	0.0541	0.0193	35.65

6.3 Vibration mode

The vibration modes are estimated by ERA, ERA/DC and PHCA method and Figure 8 shows the result from ERA/DC method. Each vibration mode is the average of 25 times where the maximum value of the individual mode was fixed by one. Up to seventh mode, the mode shape was estimated by the individual method. The first, second, third, and fifth mode were

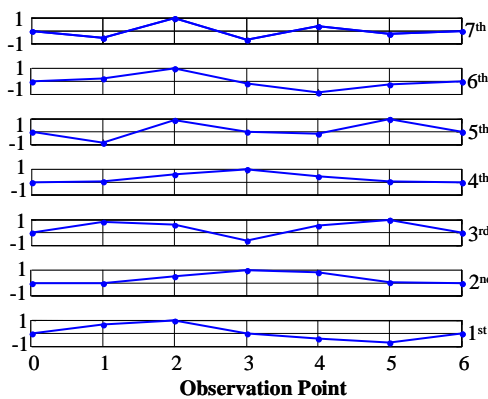


Fig.8 Estimated vibration mode by ERA/DC method (strong wind)

similar in shape of the typical larger girder bridge. The fourth mode is identical with second mode and can be treated as torsional mode. Although the sixth and seventh modes are estimated, they are not symmetrical with standard shape. This is because the number of sensor is less than the observation points. It can be pointed out that for the accuracy realization of vibration mode, number of sensor should be equal or more than the observation points. The estimated result proves that the system can estimate vibration mode effectively if sufficient number of sensor are used during the experiment. The estimated vibration mode by ERA, ERA/DC and PHCA method are similar in shape.

7. DYNAMIC CHARACTERISTICS ESTIMATION (WEAK WIND)

7.1 Frequency

The ambient vibration data, which was measured under weak and steady wind condition, has been processed to estimate the frequencies and the results obtained from ERA/DC method are shown in Figure 9. Figure shows that up to fourth mode the frequencies are estimated regularly. In contrast, the numbers of

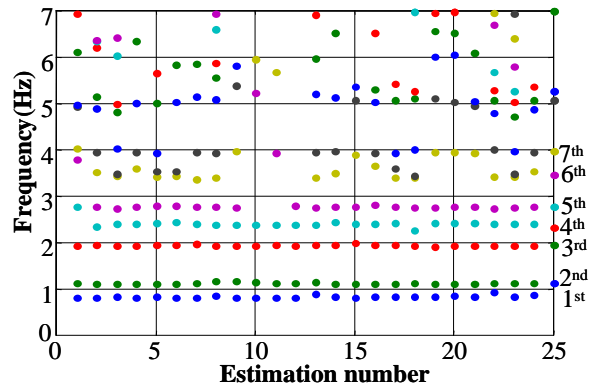


Fig.9 Estimated frequency by ERA/DC method (weak wind)

Table 5 Accuracy evaluation(weak wind)

Mode Order	Frequency(Hz)			
	Mean	Std.	C.V. (%)	
1 st	ERA	0.851	0.0658	7.74
	ERA/DC	0.851	0.0658	7.74
	PHCA	0.893	0.0704	7.88
2 nd	ERA	1.156	0.1647	14.23
	ERA/DC	1.156	0.1647	14.23
	PHCA	1.133	0.047	4.15
3 rd	ERA	1.957	0.078	3.98
	ERA/DC	1.957	0.078	3.98
	PHCA	1.975	0.0243	1.23
4 th	ERA	2.425	0.1092	4.51
	ERA/DC	2.425	0.1092	4.51
	PHCA	2.538	0.0623	2.45
5 th	ERA	2.991	0.5856	19.57
	ERA/DC	2.991	0.5856	19.57
	PHCA	2.911	0.3963	13.61
6 th	ERA	3.473	1.1907	34.27
	ERA/DC	3.473	1.1907	34.27
	PHCA	3.744	0.614	16.39
7 th	ERA	3.822	1.5938	41.69
	ERA/DC	3.822	1.5938	41.69
	PHCA	3.972	0.988	24.87

frequencies realized above 3Hz reduced significantly, as a result all the modes couldn't be observed distinctly. It can be noted that the low amplitude of ambient vibration can realize the lower mode very well since the low vibration cannot be induced the higher modes. The numerical values of estimated frequencies by ERA, ERA/DC and PHCA method has shown in Table 5. Table prepared for the mean values, standard deviation and coefficient of variation for estimated frequencies. It noted that PHCA method realized higher mean values, whereas the realized coefficient of variation is lower than other two methods.

7.2 Damping ratio

The damping ratio are estimated from the ambient vibration

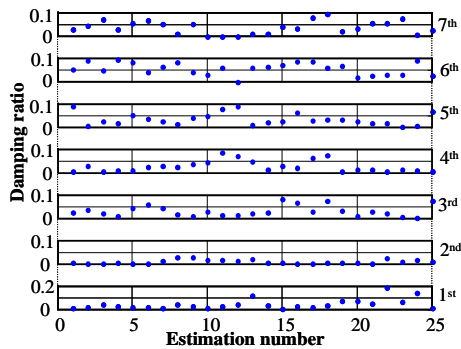


Fig.10 Estimated damping ratio by ERA/DC method (weak wind)

Table 6 Accuracy evaluation (weak wind)

Mode Order	Damping ratio			
	Mean	Std.	C.V. (%)	
1 st	ERA	0.051	0.0536	105.05
	ERA/DC	0.051	0.0536	105.05
	PHCA	0.1334	0.0711	53.31
2 nd	ERA	0.0108	0.0093	58.95
	ERA/DC	0.0108	0.0093	58.95
	PHCA	0.0727	0.0708	97.34
3 rd	ERA	0.0329	0.0225	68.31
	ERA/DC	0.0329	0.0225	68.31
	PHCA	0.0923	0.0373	40.41
4 th	ERA	0.0276	0.0244	88.46
	ERA/DC	0.0276	0.0244	88.46
	PHCA	0.0725	0.0332	45.72
5 th	ERA	0.0336	0.0226	67.35
	ERA/DC	0.0336	0.0226	67.35
	PHCA	0.0823	0.0345	41.94
6 th	ERA	0.0497	0.0279	56.12
	ERA/DC	0.0497	0.0279	56.12
	PHCA	0.1163	0.0294	25.27
7 th	ERA	0.0355	0.0247	62.85
	ERA/DC	0.0355	0.0247	62.85
	PHCA	0.0906	0.0391	43.12

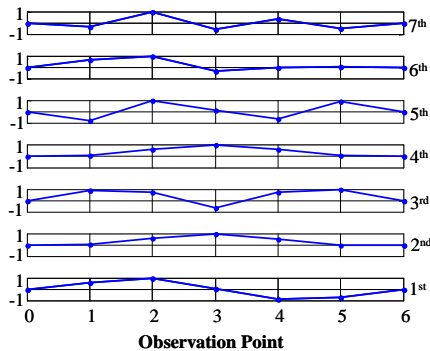


Fig.11 Estimated vibration mode by ERA/DC method (weak wind)

data of weak wind condition by ERA/DC method which is presented in the Figure 10. Comparatively higher values of damping ratio are estimated for first mode. The realized damping values are not arranged as compared to the estimated frequency. To explain more distinctly, the numerical values of the estimated damping ratio by ERA, ERA/DC and PHCA method are presented in Table 6. The results shows that the estimated damping values from PHCA method are significantly higher whereas the realized percentage of coefficient of variation is less than other two methods. The higher percentage of coefficient of variation is realized for first mode and it declined to the higher mode even for each methods.

7.3 Vibration mode

Figure 11 is plotted for the estimated vibration mode from the data, which possesses weak wind nature. In a general trend, the estimated vibration mode shapes are basically same as those are estimated from the strong wind data. This is because the average values of 25 estimation times.

8. DYNAMIC CHARACTERISTICS ESTIMATION (UNDER TRAFFIC CONDITION)

8.1 Frequency

The frequencies have been estimated using the measured data under traffic condition by various methods. The results from

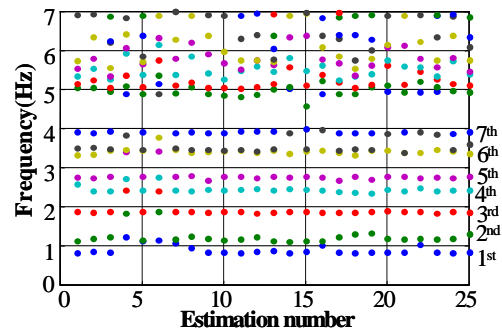


Fig.12 Estimated frequency by EAR/DC method (under traffic condition)

Table 7 Accuracy evaluation (under traffic condition)

Mode Order	Frequency(Hz)			
	Mean	Std.	C.V.(%)	
1 st	ERA	0.914	0.147	16.03
	ERA/DC	0.914	0.147	16.03
	PHCA	0.964	0.177	18.32
2 nd	ERA	1.349	0.303	22.45
	ERA/DC	1.349	0.303	22.45
	PHCA	1.353	0.402	29.73
3 rd	ERA	2.001	0.273	13.61
	ERA/DC	2.001	0.273	13.61
	PHCA	2.047	0.382	18.67
4 th	ERA	2.571	0.240	9.33
	ERA/DC	2.571	0.240	9.33
	PHCA	2.699	0.316	11.71
5 th	ERA	3.110	0.474	15.21
	ERA/DC	3.110	0.474	15.21
	PHCA	3.191	0.678	21.25
6 th	ERA	3.855	0.610	15.83
	ERA/DC	3.855	0.610	15.83
	PHCA	3.997	0.731	18.31
7 th	ERA	4.326	0.703	16.24
	ERA/DC	4.326	0.703	16.24
	PHCA	4.571	0.678	14.84

ERA/DC method are provided in Figure 12. In general, it is observed that there is a lack of estimation on lower mode frequency. In contrast, the number of realized frequencies above the 4Hz increased significantly since the moving vehicle can induces the higher mode frequently. To evaluate the accuracy over three methods, the estimated frequencies are numerically presented on Table 7. According to the results in the table, PHCA method realized higher percentage of coefficient of variation as well as higher means values of frequencies. Overall, the realized coefficient of variation increased noticeably than the results obtained from other two types of data, which is due to the averaging effect of individually estimated values.

8.2 Damping ratio

The damping ratio is estimated from the ambient vibration data under traffic condition are graphically presented in Figure 13. The figure reveals that the values of estimated damping for first mode is comparatively high. The damping values for higher mode seems to be more arranged due to the effect of vehicle loading influences. For comparison, the estimated values can be seen from the Table 8, which reveals that the PHCA method realized the higher mean values whereas the coefficient of variation is less than other two cases.

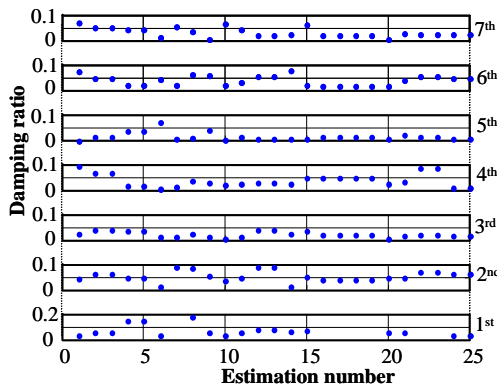


Fig.13 Estimated damping ratio by EAR/DC method (under traffic condition)

Table 8 Accuracy evaluation (under traffic condition)

Mode Order	Damping ratio			
	Mean	Std.	C.V. (%)	
1 st	ERA	0.0679	0.0359	52.83
	ERA/DC	0.0679	0.0359	52.83
	PHCA	0.1934	0.0613	31.68
2 nd	ERA	0.0499	0.0236	47.37
	ERA/DC	0.0499	0.0236	47.37
	PHCA	0.1996	0.0714	35.77
3 rd	ERA	0.0298	0.0253	84.85
	ERA/DC	0.0298	0.0253	84.85
	PHCA	0.1051	0.0279	26.49
4 th	ERA	0.0299	0.0206	68.77
	ERA/DC	0.0299	0.0206	68.77
	PHCA	0.0890	0.0436	48.54
5 th	ERA	0.0233	0.0172	73.83
	ERA/DC	0.0233	0.0172	73.83
	PHCA	0.0685	0.0324	47.37
6 th	ERA	0.0274	0.0146	53.33
	ERA/DC	0.0274	0.0146	53.33
	PHCA	0.0581	0.0199	34.35
7 th	ERA	0.0212	0.0128	60.62
	ERA/DC	0.0212	0.0128	60.62
	PHCA	0.0541	0.0193	35.65

8.3 Vibration mode

The estimated results for vibration mode by ERA/DC method are shown in Figure 14. This Figure is plotted for the average values of 25 estimation times, which shows that the estimated vibration modes are identical in shape with the results from other two cases of data. This signifies that the multipoint observation can estimate the vibration mode accurately even though the ambient conditions are different.

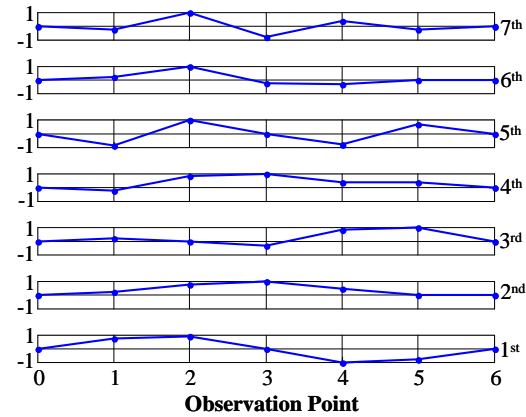


Fig.14 Estimated vibration mode by EAR/DC method (under traffic condition)

8.4 Performance evaluation for ERA, ERA/DC and PHCA method

The performance of three methods such as ERA, ERA/DC and PHCA method can be evaluated based on the operational time as well as estimation accuracy. In case of ERA/DC method the computational complexity reduces for the smaller size of the Hankel matrix as it is derived from the correlation of covariance matrix and shortened the operation time as well. The shorter calculation time is needed in order of ERA/DC, ERA, and PHCA method. ERA, ERA/DC maintained same level of estimation accuracy but better than PHCA method. In general, we can arrange the applied theories in descending order of best performance as (1) ERA/DC, (2) ERA and (3) PHCA method respectively.

9. CONCLUSIONS

How the dynamic characteristics (frequency, damping ratio, and vibration mode) of bridges can be estimated by using three different stochastic realization theories under ambient vibration has been shown in this study. The proposed methods have been successfully applied to existing steel langer girder bridge under three different cases of ambient vibration: (a) strong wind condition, (b) weak wind condition and (c) under traffic condition. The results from various cases of ambient vibration data illustrate the usefulness of the methods to estimate the dynamic characteristics of the existing bridge and leads to the following conclusions.

(1) The variation in results under various kind of ambient vibration proves the influence of ambient condition on estimation accuracy. High amplitude and stationary (strong wind induced) ambient vibration can realize the better estimation accuracy which is recommended as preferred ambient condition for multipoint measurement.

(2) The weak wind induced ambient vibration can estimate the lower mode effectively but incase of higher mode the estimation accuracy declines since the low vibration cannot induced the higher mode.

(3) The ambient vibration data measured under traffic condition shows a lack of estimation accuracy in lower modes. On the other hand, the moving vehicle induced high frequency leads to frequent estimation of higher mode but do not show consistency, as the excitation are not steady in nature.

(4) As a realization theory ERA, ERA/DC method realized the same performance on estimation accuracy. Even though for some aspect PHCA method realized same accuracy but in a general trend its performance can be treated as inferior than other two methods. Especially, ERA/DC method has the advantages for its simple algorithm and ability to provide accurate estimation with fast computational speed.

(5) In order to perform automatic ambient vibration measurement; ambient vibration intensity and uniformity in amplitude should be taken in consideration.

In this research, we performed the identification considering the various effects of external forces as well as used various realization theories to judge the estimation accuracy. And it was not targeted to identify the quantity or the location of damage. To do this, the environmental condition such as temperature variation, effect of surrounding environment was not considered during the observation period.

ACKNOWLEDGEMENT

The authors would like to express their gratitude to the Public Works Department of Nagasaki Prefecture and Nagasaki Public Works Office for giving us the opportunity to conduct a series of measurements.

References

- 1) Sohn, H., Farrar, C. R., Hemez, F. M., Shunk, D. D., Stinemates, D. W. and Nadler, B. R., A review of structural health monitoring literature: 1996-2001. *Los Alamos National Laboratory Report LA-13976-MS*, 2003.
- 2) Farrar, C. R., and Worden, K., An introduction to structural health monitoring, *Phil. Trans. Soc.*, Vol. 365, pp.303-315, 2007.
- 3) Lee, J. W., Kim, J. D., Yun, C. B., Yi, J. H., Shim, J. M., Health-monitoring method for bridges under ordinary traffic loadings, *Journal of Sound and Vibration*, Vol. 257(2), pp.247-264, 2002.
- 4) Peeters, B. and Roeck, G. D., Stochastic system identification for operational modal analysis: a review, *Journal of Dynamic System, Measurement, and Control*, Vol. 123, pp.659-667, 2001.
- 5) Quek, S. T., Wang, W. and Koh, C. G., System identification of linear MDOF structures under ambient excitation, *Earthquake Eng. and Struct. Dyn.* Vol. 28, pp.61-77, 1999.
- 6) Huang, C. S., Structural identification from ambient vibration measurement using the multivariate AR model, *Journal of Sound and Vibration*, Vol.241 (3), pp.337-359, 2001.
- 7) Okumatsu, T., Okabayashi, T., Fusamae, S., Funabara, Y., and Oiwane, K., High accurate estimation of structural dynamic characteristics by two-step structural identification method, *Journal of Structural Engineering*, Vol.52A, pp.227-237, 2007.
- 8) Okabayashi, T., Okumatsu, T. and Nakamia, Y., Experimental study on structural damage detection using the high accurate structural vibration-estimation system, *Journal of Structural Engineering*, Vol.51A, pp.479-490, 2005.
- 9) Okumatsu, T., Okabayashi, T., Jawaid, B. A., Tashiro, D. and Deguchi, K., Monitoring of vibration characteristics of the kabashima bridge by mobile communication system, *Journal of Structural Engineering*, Vol.53A, pp.844-852, 2007.
- 10) Jimin, H. and Zhi-Fang, F., *Modal Analysis*, Butterworth-Heinmann, 2001.
- 11) Hung, C. F., Ko, W. J. and Peng, Y. T., Identification of modal parameters from measured input and output data using a vector backward auto-regressive with exogenous model, *Journal of Sound and Vibration* Vol.276, pp.1043-1063, 2004.
- 12) Carden, E. P. and Brownjohn, M. W., ARMA modeled time-series classification for structural health monitoring of civil structure, *Mechanical System and Signal Processing*, Vol.22, pp.295-314, 2008.
- 13) Yang, Q. J., Zhang, P. Q., Li, C. Q. and Wu, X. P., A system theory approach to multi-input multi-output modal parameters identification methods, *Mechanical System and Signal Processing*, Vol.8 (2), pp.159-174, 1994.
- 14) Kang, J. S., Park, S. K., Shin, S. and Lee, H. S., Structural identification in time domain using measured acceleration, *Journal of Sound and Vibration*, Vol.288, pp.215-234, 2005.
- 15) Lehmans, L. and Auwerar, H. V., Modal testing and analysis of structures under operational conditions: industrial applications, *Mechanical System and Signal Processing*, Vol.13 (2), pp.193-216, 2008.
- 16) Ewins, D. J., *Modal Testing: Theory and Practice*, John Wiley and Sons Inc. New Work, 1994.

- 17) Juang, J. N., *Applied System Identification*, Prentice Hall, 1994.
- 18) Nagayama, T., Abe M., Fujino, Y., and Ikeda, K., Structural identification of a non proportionally damped system and its application to full-scale suspension bridge, *Journal of Structural Engineering*, Vol. 131(10), pp. 1536-1545, 2005.
- 19) Siringoringo, D. M. and Fujino, Y., System identification of suspension bridge from ambient vibration response, *Engineering Structures*, Vol. 30(2), pp. 462-477, 2008.
- 20) Okauchi, I., Miyata, T., Tatsumi, M. and Sasaki, N., Field vibration test of long - span cable-stayed bridge using large exciters, *Structural/Earthquake Engineering, JSCE*, Vol.14, pp.83-93, 1997.
- 21) Farrar, C. R., and James III, G. H., System identification from ambient vibration measurement on a bridge, *Journal of Sound and Vibration*, Vol.205 (1), pp.1-18, 1997.
- 22) Jawaid, B. A., Okabayashi, T., Ali, M. R., and Okumatsu, T., Automated dynamic characteristics estimation under ambient vibration by block companion form realization, *Journal of Structural Engineering*, Vol.54A, pp.189-198, 2008.
- 23) Juang, J. N. and Pappa, R. S., An eigensystem realization algorithm for modal parameter identification and model reduction, *Journal of Guidance, Control and Dynamics* Vol.8 (5), pp.620-627, 1985.
- 24) Juang, J. N., Cooper, J. E. and Wright, J. P., An eigensystem realization algorithm using data correlations (ERA/DC) for modal parameter identification, *Control-Theory and Advanced Technology* Vol.4 (1), pp.5-14, 1988.
- 25) Kung, S., A new identification and model reduction algorithm via singular value decomposition, *12th Asiomar Conference on Circuit, Systems and Computers*, pp.705-714, 1978.

(Received September 18, 2008)